RAA 2015 Vol. **15** No. **11**, 1867–1880 doi: 10.1088/1674–4527/15/11/009
http://www.raa-journal.org *http://www.iop.org/journals/raa*

***R**esearch in*
***A**stronomy and*
***A**strophysics*

Panoramic camera on the Yutu lunar rover of the Chang'e-3 mission

Jian-Feng Yang[1], Chun-Lai Li[2], Bin Xue[1], Ping Ruan[1], Wei Gao[1], Wei-Dong Qiao[1], Di Lu[1], Xiao-Long Ma[1], Fu Li[1], Ying-Hong He[1], Ting Li[1], Xin Ren[2] and Xing-Tao Yan[1]

[1] Lunar and Deep Space Exploration Technology Laboratory of Xi'an Institute of Optics and Precision Mechanics, Chinese Academy of Sciences, Xi'an 710068, China; *ytop31@163.com*
[2] National Astronomical Observatories, Chinese Academy of Sciences, Beijing 100012, China

Received 2014 July 21; accepted 2015 April 7

Abstract The Chang'e-3 panoramic camera, which is composed of two cameras with identical functions, performances and interfaces, is installed on the lunar rover mast. It can acquire 3D images of the lunar surface based on the principle of binocular stereo vision. By rotating and pitching the mast, it can take several photographs of the patrol area. After stitching these images, panoramic images of the scenes will be obtained. Thus the topography and geomorphology of the patrol area and the impact crater, as well as the geological structure of the lunar surface, will be analyzed and studied. In addition, it can take color photographs of the lander using the Bayer color coding principle. It can observe the working status of the lander by switching between static image mode and dynamic video mode with automatic exposure time. The focal length of the lens on the panoramic camera is 50 mm and the field of view is $19.7^\circ \times 14.5^\circ$. Under the best illumination and viewing conditions, the largest signal-to-noise ratio of the panoramic camera is 44 dB. Its static modulation transfer function is 0.33. A large number of ground testing experiments and on-orbit imaging results show that the functional interface of the panoramic camera works normally. The image quality of the panoramic camera is satisfactory. All the performance parameters of the panoramic camera satisfy the design requirements.

Key words: Moon — methods: observational — techniques: image processing — high angular resolution

1 INTRODUCTION

The three phases of China's lunar exploration plan include orbiting, landing and sample return. After the successful launch of the Chang'e-1 and Chang'e-2 satellites, the Chang'e-3 (CE-3) mission, which was made up of the first lander and rover in China's lunar exploration program, was charged with a number of science missions to explore the Moon's surface (Sun et al. 2013; Ouyang 2006). The Yutu lunar rover was the first lunar rover launched and controlled by China (Wang et al. 2014). It has undertaken many scientific goals, such as imaging the lunar surface and carrying out geological structure investigation and detection (Ouyang 2005). The CE-3 panoramic camera, which operates in a similar way to a rabbit's eyes, is an important payload on Yutu. It is composed of two cameras with identical functions, performances and interfaces, and is installed on the lunar rover mast (Ip et al. 2014; Li et al. 2014). It can acquire 3D photos of the lunar surface based on the principle of binocular stereo vision. With the rotation and pitching of the mast, it can take multiple photographs of the scenes. After stitching these images, panoramic images of the scenes have been obtained. These images are used to investigate the geomorphology of the patrol area, impact craters, lunar geological structure, and so on (Dai et al. 2014). Meanwhile, both monochrome and color photos of the lander have been taken by the panoramic camera. From these photos, the working state of the lander was constantly monitored. In order to satisfy the weight, volume, performance, lifetime and other requirements of the spacecraft's payload, the optical, structural, thermal and electronic design of the CE-3 panoramic camera had to overcome many technical difficulties. This camera contributed to the successful completion of the CE-3 mission, and advanced engineering expertise in camera design related to lunar and deep space exploration.

This paper introduces the panoramic camera and its on-orbit check out results in detail. Section 2 gives the technical parameters of the panoramic camera. Section 3 provides the composition of the panoramic camera. Section 4 introduces the system design of the panoramic camera. In Section 5, calibration experiments related to the panoramic camera are summarized. Section 6 gives some on-orbit images of the panoramic camera.

2 TECHNICAL PARAMETERS

2.1 Camera Parameters

According to user requirements and lunar imaging characteristics, the technical parameters of the panoramic camera are shown in Table 1. It must be able to endure the low temperature on the Moon. It should be able to clearly image objects as distances from 3 m to infinity in the visible spectral range. During the actual working state, it takes color photographs of the lander using color mode, and monochrome pictures of other scientific exploration targets using panchromatic mode. In the panchromatic mode, the data in every four pixels are merged into one pixel (2×2 binning). At this point, the spatial resolution of the camera will decline, but the image quality can be further improved. Besides meeting the requirements of field of view and the focal length, the static modulation transfer function (MTF) of a designed optical system must be greater than 0.2. MTF is an important evaluation standard for the imaging system, which is numerically between 0 and 1. For a scientific imaging camera, its static MTF must be larger than 0.2 to ensure favorable imaging results. In order to stay within restrictions of the whole weight of the CE-3 payload, the total weight of the two cameras must be less than 0.65 kg.

2.2 Sensor Performance Parameters

The image sensor in each panoramic camera is a Complementary Metal Oxide Semiconductor (CMOS) chip produced by DALSA. The main performance parameters of the sensor are shown in Table 2. Each pixel size is 7.4 μm × 7.4 μm, which effectively guarantees the spatial resolution of the panoramic camera. The largest frame frequency is 62 fps, which ensures high-speed transfer of data and the ability to work in video mode. The sensor has a wide dynamic range and spectral response range. As shown in Figure 1, it has different responses to wavelength bands R, G and B. This will lead to chromatism in color images taken by the panoramic camera. Therefore, the optical design and subsequent processing should be taken into account to ensure the consistency of images.

3 COMPOSITION OF THE PANORAMIC CAMERA

The panoramic camera is actually a set of artificial stereo imaging equipment, whose two cameras are similar to human eyes. The principle of binocular stereo vision used in the eyes of humans is shown

Table 1 Main Technical Parameters of the Panoramic Camera

Items	Parameters
Spectral range	$420\ \mathrm{nm} \sim 700\ \mathrm{nm}$
Color	Red; Green; Blue (R; G; B)
Image mode	Color mode; Panchromatic mode (Can be switched)
Normal imaging distance (m)	$3 \sim \infty$
Effective pixel numbers	2352×1728 (Color mode); 1176×864 (Panchromatic mode)
Field of view	$19.7° \times 14.5°$
Focal length	50 mm
Optical system static MTF	$\geqslant 0.2$
Quantitative values (bit)	10
Signal to noise ratio S/N (dB)	$\geqslant 40$ (Under the best illumination and viewing conditions) $\geqslant 30$ (Albedo: 0.09, Angle of the Sun: $19.7°$)
Distance between two cameras' optical axis	270 ± 2 mm
Average power consumption (W)	$\leqslant 5$
Weight (kg)	$\leqslant 0.65$ (Two cameras')

Table 2 Main Performance Parameters of the Sensor

Items	Parameters
Sensor mode	IA-G3 DALSA
Pixel number	2352×1728
Pixel size	7.4 μm $\times$ 7.4 μm
Frame frequency	62 fps
Spectral response range	400 nm $\sim$ 750 nm
Full trap charge	60 ke
Dynamic range	57 dB

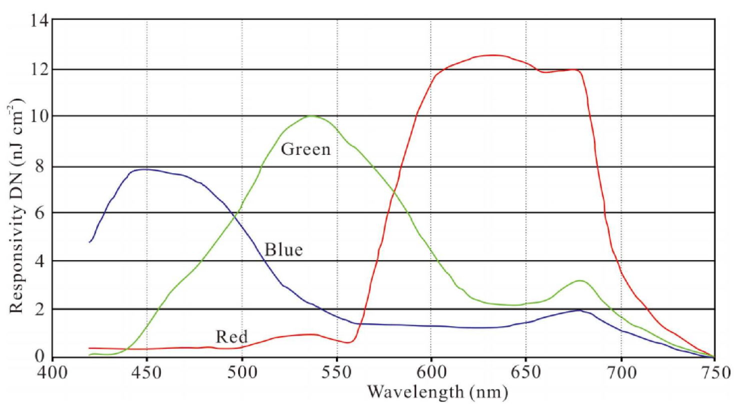

Fig. 1 Spectral response curves of the panoramic camera sensor.

in Figure 2 (left). When the eyes gaze at point A, the visual axis of the two eyes will instinctively intersect at this point. The intersection angle is γ. At the same time, for a point B (near A), the intersection angle of the two eyes' visual axis is $\gamma + d\gamma$. As the intersection angle of the visual axis at point B is larger than at point A, point B is perceived as being closer to the eyes than point A. On the two retinas, the difference in coordinates between the image at point A is $P_A = a - a'$, and the difference in coordinates between point B is $P_B = b - b'$. The difference in coordinates between

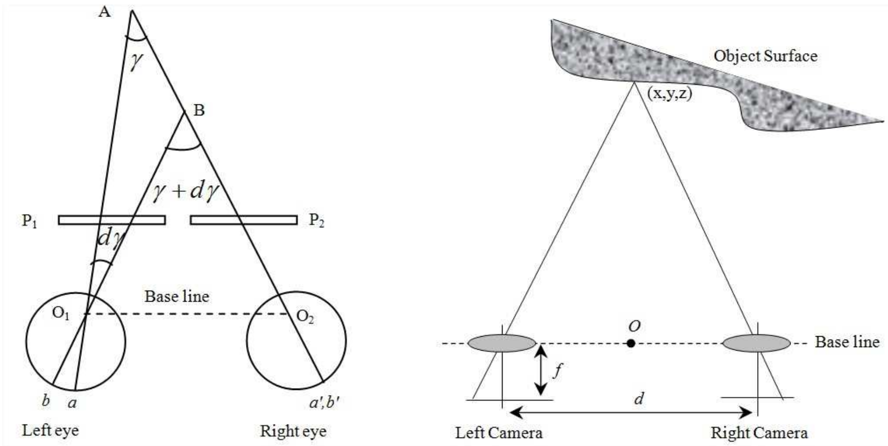

Fig. 2 Schematic diagram of binocular stereo imaging used by human eyes and stereo imaging used by the panoramic camera.

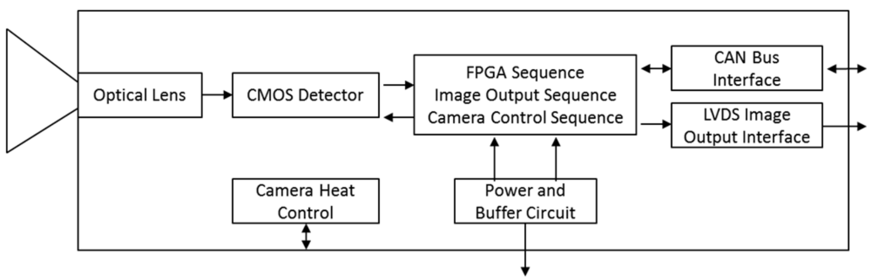

Fig. 3 Composition diagram of the panoramic camera.

the two points is $p = P_A - P_B = a - b$, where p is called the horizontal parallax difference or physiological parallax. This is why the eyes can distinguish nearby objects from those that are far. Similarly, if we place a plane in front of each retina to record each image and remove point A and B, we can also distinguish point A from B by observing the images on the planes. The reason is that the difference in horizontal parallax between A and B still exists. According to the principle above, if we place two cameras at positions P_1 and P_2 to image the same object at the same time, we can get two images of each scene, as shown in Figure 2 (right). By measuring the coordinates of a homologous point in the two images, we can recover the depth or distance to the target. This process should be completed by special calibration experiments of a panoramic camera to obtain effective camera parameters.

Each single camera that is part of a panoramic camera includes the components of an optical system, structural system, electronic system and thermal control system. The electronic system includes a CMOS sensor, camera power, buffer circuit, sequential control Field Programmable Gate Array (FPGA), camera control input interface (Controller Area Network (CAN) bus), image output interface (Low Voltage Differential Signaling (LVDS)), etc. Figure 3 shows the composition schematic diagram of the panoramic camera.

4 DESIGN OF THE PANORAMIC CAMERA

4.1 Optical System Design

According to the technical parameters, the field of view of each camera should be $19.7^\circ \times 14.5^\circ$. The camera's focal length is 50 mm. For normally imaging both near and far objects, and ensuring the signal strength, the F number of the optical system is 10. It is a system with a large F number, so the system has a large depth of field. For balancing the weight and imaging quality of the optical system, a structure with four lenses was chosen. Each lens only has primary aberration and system tolerance range is wide, which ensures an easier assembly and good temperature adaptability. A glass covering and filter were also added to protect and improve the optical system. A schematic diagram of the structural layout of the system is shown in Figure 4. The total length, back focal length and system diameter are 63.05, 41.05 and 14 mm respectively. As shown in Figure 5, MTF of the designed optical system in each field is close to the diffraction limit and is over 0.52 at the Nyquist frequency. This ensures good imaging quality at both the center and edge of the field.

4.2 Structural System Design

The panoramic camera structure includes the optical lens and a focal plane control box. In accordance with requirements of the working environment and guaranteeing the image quality of the optical system, the key point in the structural design is the integration of the optical, structural, electronic and thermal control systems to make the camera lightweight. The optical lens is designed as an independent part. The hood material is aluminum alloy. The tube material is titanium alloy with high stiffness and a small thermal expansion coefficient. The optical lenses are fixed by a screw clamping ring. The material that makes the focal plane control box is aluminum alloy. The connection between the detector and circuit board is directly welded. The circuit board is fixed on the shell of the control box. A photo of the panoramic camera is shown in Figure 6. Each single camera size is 90 mm$\times$110 mm$\times$110 mm. The total weight of the two cameras is 0.64 kg. Both of them satisfy the requirements for weight and volume.

4.3 Electronics Design

A schematic diagram illustrating the electronics design is shown in Figure 7. The sensor IA-G3 transforms the image signal directly to FPGA. FPGA is the control core of the camera and transforms the output image through an LVDS serial interface circuit. The control of the camera is dependent on the payload electric cabinet. This design reduces the power consumption and volume required for this system. In order to improve the adaptability for changes in target and light intensity, the camera should control the brightness of images from different scenes. Thus, FPGA is designed with two kinds of control functions: automatic and manual exposure mode. The former automatically changes the exposure time by setting the best average exposure time, while the latter directly acquires the exposure time that comes from the ground control system. The stability, compactness and quickness of the designed electronics system guarantee the acquisition control, transmission and storage ability of the panoramic camera image. It works as the central nervous system for the whole camera.

4.4 Thermal Control Design

As there is no atmosphere on the Moon, the temperature difference between day and night is very large. Therefore, the panoramic camera should be able to adapt to this large temperature change. In other words, it needs to operate in a wide range of environmental temperatures, so both panoramic camera A and B have a temperature sensor to constantly monitor the focal plane temperature. Two kinds of thermal measuring devices are utilized in this scheme. One covers the surface of the optical

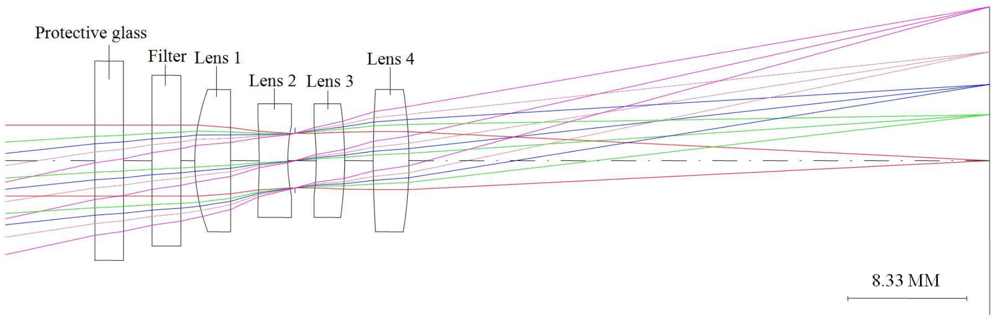

Fig. 4 Layout of the optical system.

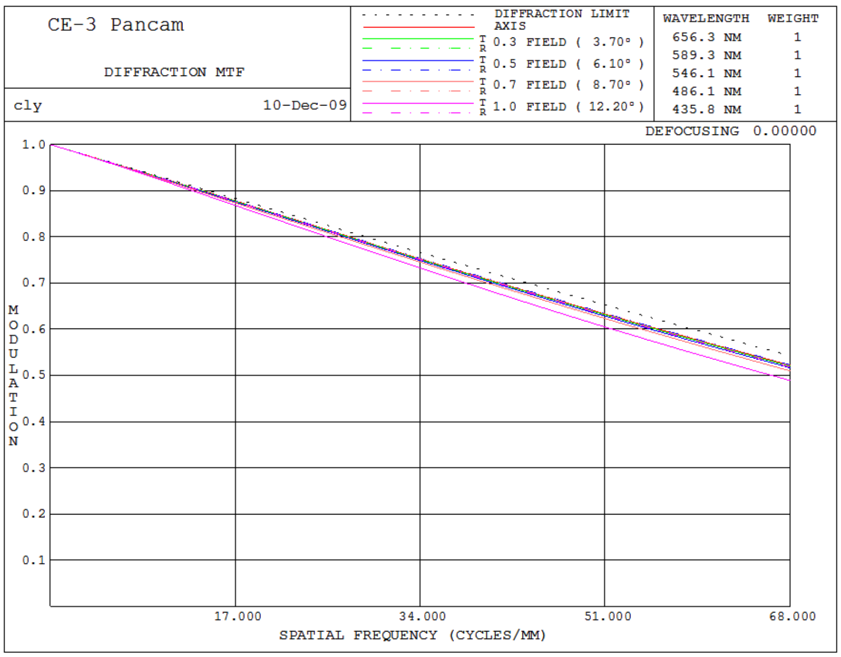

Fig. 5 MTF of the designed optical system.

lens structure with multilayer insulation materials, and the other is Optical Solar Reflector material with low absorption rate and high emissivity material that is pasted on the upper part of the focal plane box. We have carried out various ground testing experiments, such as 100 hours of continual experimentation, a high and low temperature cycle experiment and a vacuum simulation experiment. The panoramic camera works normally in such experiments that have a $-25°C\sim+55°C$ temperature range, and its image quality is consistently good.

5 CALIBRATION AND PARAMETER TESTING

The purpose of calibration is to calibrate the parameters of the apparatus, in order to eliminate the various errors and inconsistencies produced by the instrument and make the imaging data produced by the instrument more accurate. The calibration of the panoramic camera includes: dark current

Fig. 6 Photo of the panoramic camera.

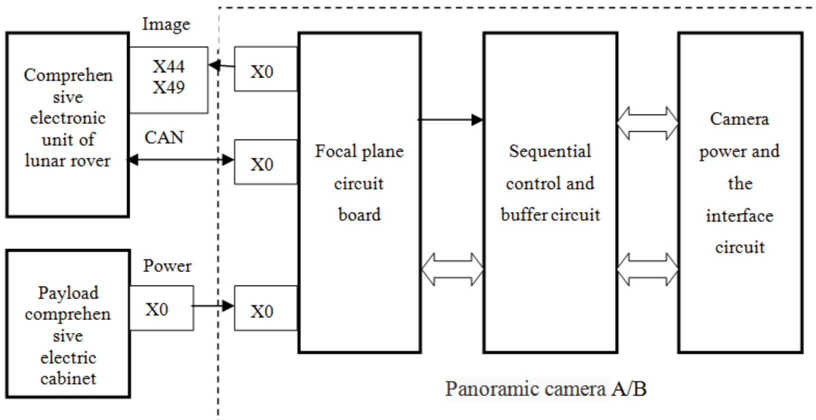

Fig. 7 Schematic diagram of the electronic system associated with the panoramic camera.

Table 3 Main Equipment Used in the Panoramic Camera Calibration

Equipment name	Model	Main technical indicators
Spectral radiation meter	Fieldspec Pro UV/VNFR	Spectral range: 350 nm ∼ 1050 nm; Spectral resolution: 3 nm; Quantitative level: 16-bit
Integrating sphere system	Labsphere XTH- 2000	Provide uniform plane light source; Ball diameter is 1.65 m; Open aperture is 550 mm; Adjustable; Uniformity $> 99\%$.
Standard color light box	D65 light box	Produce D65 light source
Standard color card	Color Checker	X-rite, standard 24 color
Object	—	White board, the national flag, striped cloth

calibration, relative radiation calibration, mode normalization and color calibration. The purpose of parameter testing is to check the main parameters of the fabricated panoramic camera. It includes checking of geometric distortion, linearity, focal length, MTF, etc. All of these experiments have been meticulously performed. For brevity, let us briefly introduce the major ones below. The main pieces of equipment used in the calibration experiments are shown in Table 3.

5.1 Dark Current Calibration

The camera's dark current is the detector's response without radiation input. It directly affects the contrast ratio of the camera's image. The procedure is to cover the panoramic camera lens with its cap to ensure no incident radiation triggers the sensor, change the working modes, save 25 dark images in each mode, calculate the numerical values of the dark current coefficient matrix, and draw the relationship curve between dark current and exposure time. The mathematical model of

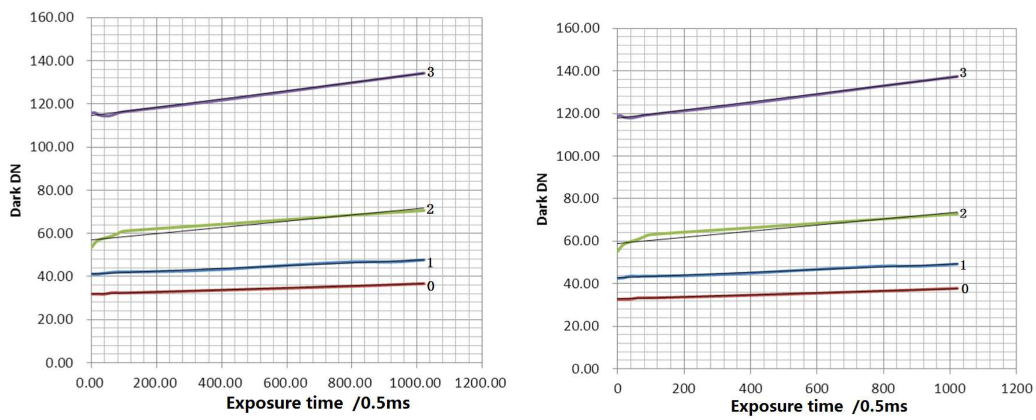

Fig. 8 Relationships between dark current and exposure time for panoramic camera A (*left*) and B (*right*).

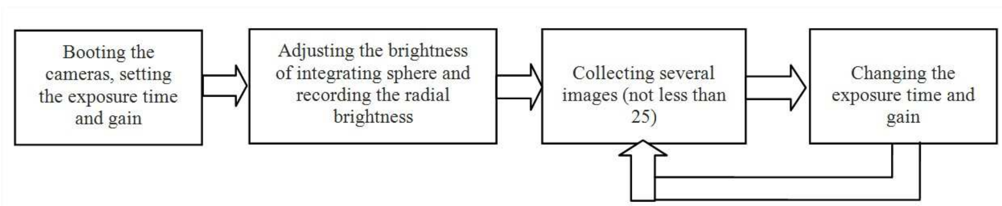

Fig. 9 Steps in the panoramic camera relative radiation calibration experiment.

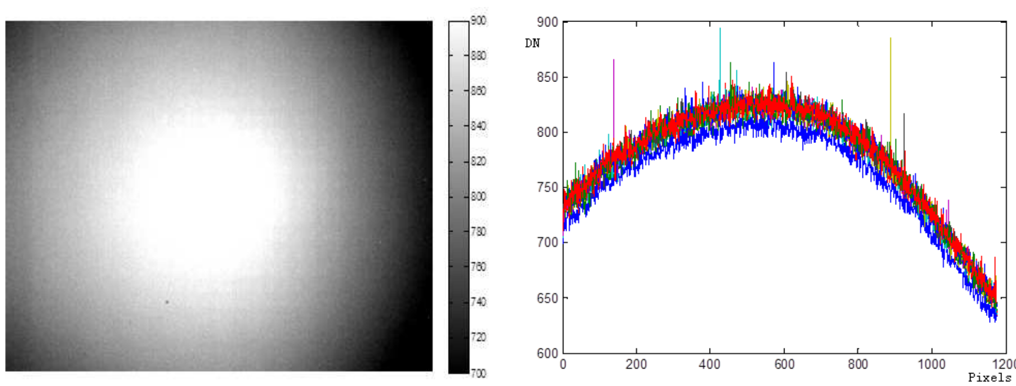

(a) The image before flat field correction. (b) DN value curve of middle row pixels.

Fig. 10 The image of channel R before flat field correction.

dark current calibration can be described as calculating the average dark current for each pixel; calculating the average dark current of the whole CMOS sensor; calculating the dark current RMS for each pixel. The dark current calibration results of the panoramic camera are shown in Figure 8, where the numbers 0, 1, 2 and 3 denote different gain settings. The difference between dark current values of the shortest and the longest exposure time is very small. To eliminate the dark current interference and improve contrast in the image, the component of dark current should be subtracted.

5.2 Relative Radiation Calibration

The goal of relative radiation calibration (flat field correction) is to eliminate the response inconsistencies between CCD or CMOS pixels (Hu & Zhang 2007). Specific steps in relative radiation calibration are shown in Figure 9. The main equipment is an integral sphere. According to the requirement, the uncertainty in the panoramic camera's relative calibration should be better than 3%. The results of the flat field correction are shown in Figures 10 and 11. To enhance contrast, a DN value has been chosen between 700 and 900. Figure 11 demonstrates the validity of relative radiation calibration. In different working modes (with different exposure times, gain setting and DN values from 200 to 900), the uncertainty in flat field correction of camera A and B is less than 1.38% and 1.23% respectively.

5.3 Mode Normalization

According to the user's requirement, the relative changes in the images taken using different working modes should be consistent, so we have implemented mode normalization rather than absolute radiometric calibration. The basis of mode normalization is the linearity in the panoramic camera response (Gao et al. 2009). The camera's linearity is the relationships between DN values and exposure times, which are shown in Figure 12. Here R, G, G, B denote the responses of each physical pixel after the color filter array (CFA) which will be introduced in Section 5.4 and shown in Figure 13. According to Figure 11, the linearity in the panoramic camera response is better than 99%, so the difference in the absolute radiometric calibration coefficient between different working modes is very small and the calibration correction coefficient matrix can be simplified into that of one mode. In this experiment, we chose the working mode with a 40 ms exposure time and gain setting of 1. This is the meaning of mode normalization.

5.4 Color Calibration

Based on the Bayer color coding principle, the panoramic camera can take color photographs of the lander. The schematic diagram is shown in Figure 13. It uses a single CMOS for a digital still camera with a color filter array (CFA) placed in front of the image sensor array. Each physical pixel of the sensor can collect one of three primary color components (Red (R), Green (G) and Blue (B)). In order to get the full color image, three color components (R, G and B) must be known. Therefore, the two missing color values of each pixel must be estimated from adjacent pixels. This process is known as color interpolation or demosaicing. A color interpolation algorithm is related to the pattern of the CFA. The CFA pattern of the panoramic camera shown in Figure 14 is a Bayer pattern. As the detector response curve (shown in Fig. 1) is different from the International Commission on Illumination (CIE) 1931 chromaticity diagram (shown in Fig. 15), chromatism will exist in color images taken by the panoramic camera. In order to correct this chromatism, a color calibration experiment must be carried out (Valous et al. 2009). After calculating the white balance coefficient and color correction coefficient matrix, the color value of the camera image will be restored into the standard color value. This work is an important part of the panoramic camera calibration. Steps in the panoramic camera color calibration experiment are shown in Figure 16.

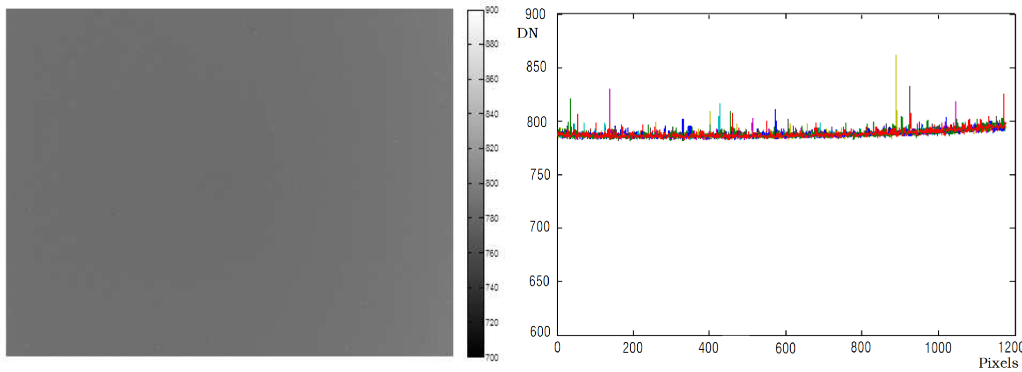

(a) The image after flat field correction. (b) DN value curve of middle row pixels.

Fig. 11 The image of channel R after flat field correction.

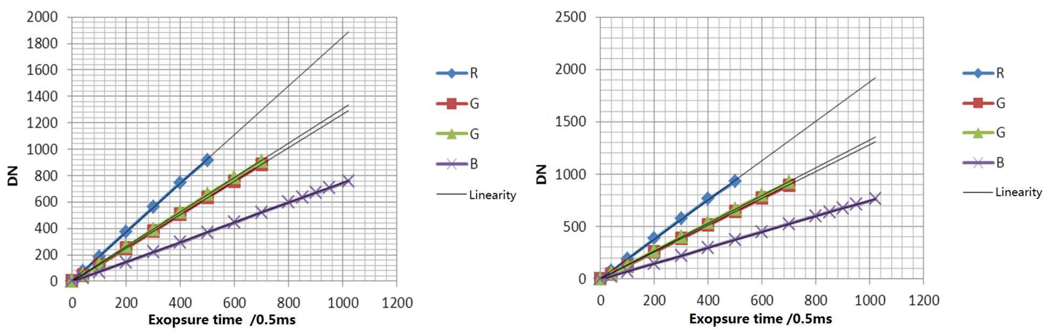

Fig. 12 The linearity of panoramic camera A (*left*) and B(*right*).

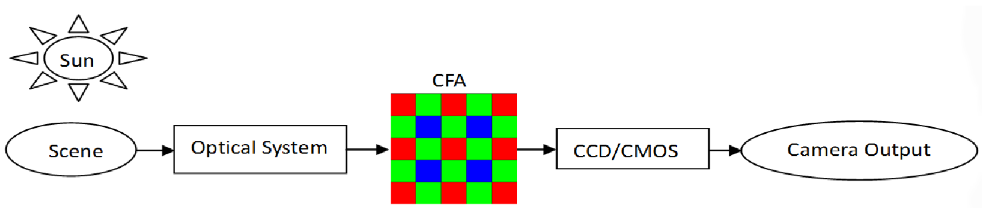

Fig. 13 Schematic diagram of the panoramic camera's color imaging mode.

Figure 17 is the comparison between the color images taken by the panoramic camera before and after the color correction. The color in Figure 17(b) is much better than that in Figure 17(a). The results of the ground test and calibration experiments show that the panoramic camera meets the general requirements and satisfies the demand of color imaging. Ren et al. have dedicated more scrutiny to the color calibration of the panoramic camera and terrain camera. More specific information and the quantitative white balance coefficient and color correction coefficient matrix calculation method can be referenced there (Ren et al. 2014).

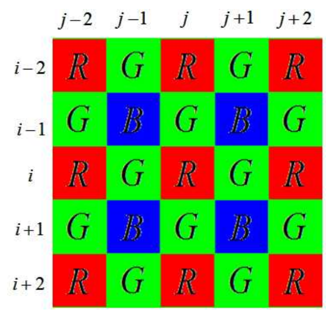

Fig. 14 Bayer pattern CFA.

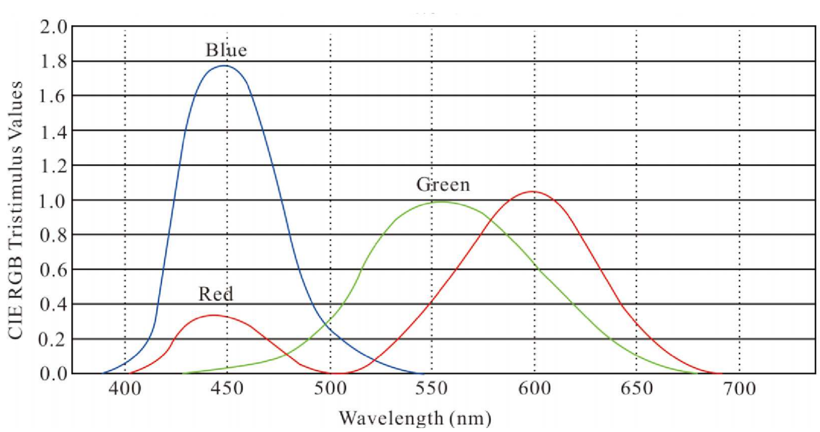

Fig. 15 CIE 1931 standard observer color matching function curves.

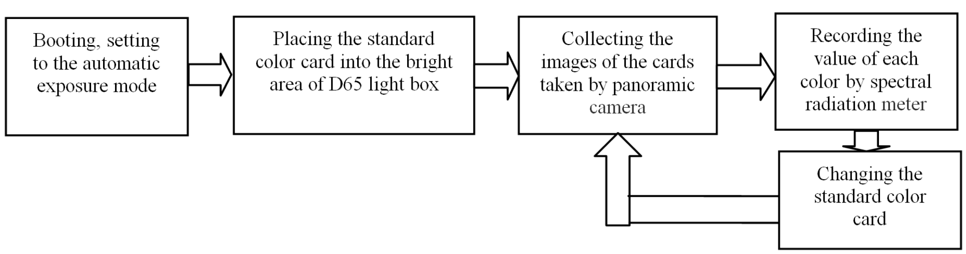

Fig. 16 Steps in the panoramic camera color calibration experiment.

5.5 Parameter Testing

The results of geometric distortion checking shows that the distortion of the panoramic camera is less than 0.05%, which is negligible. The focal lengths of panoramic camera A and B are 50.10 mm and 50.08 mm respectively. The MTF of panoramic camera A and B are 0.32 and 0.33 respectively. All these parameters satisfy the design requirements.

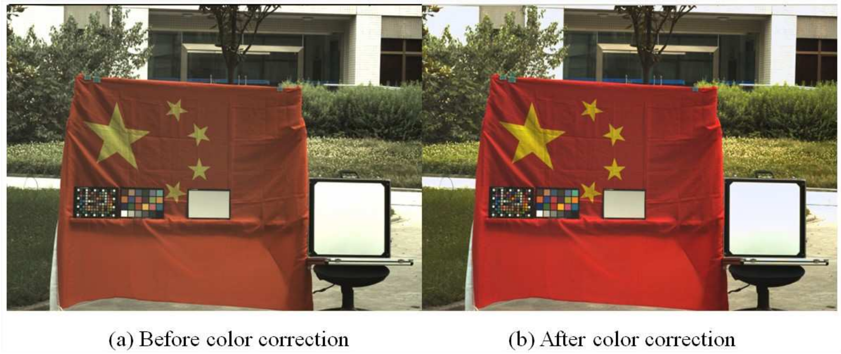

Fig. 17 Color images of a flag taken by the panoramic camera.

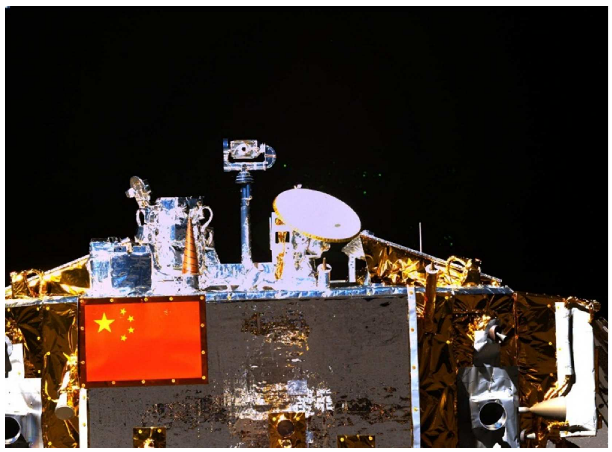

Fig. 18 A photo of the upper part of the lander taken by the panoramic camera at working point D.

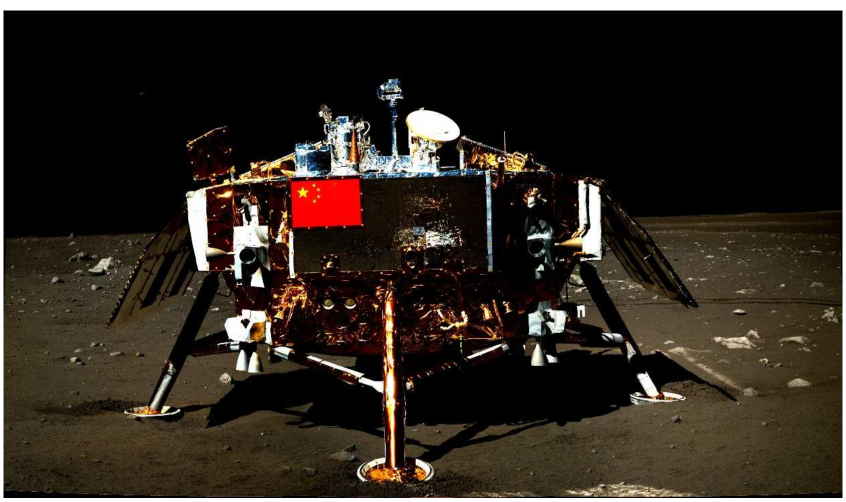

Fig. 19 A panoramic image of the lander (stitched from six images of the scene).

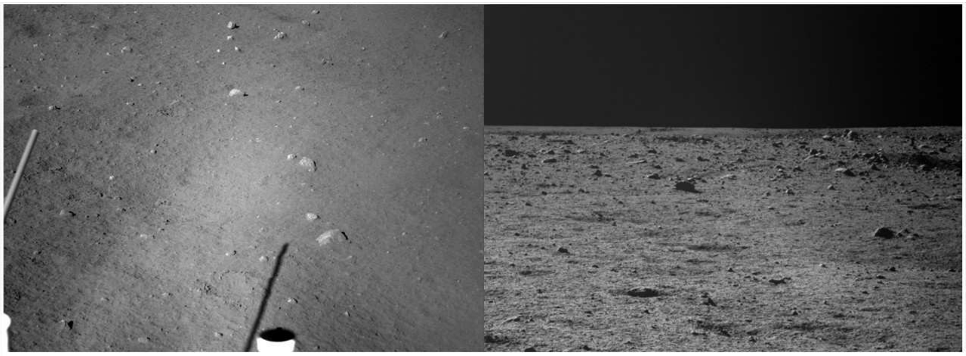

(a) Near objects (b) Far objects

Fig. 20 Photos of the patrol area.

6 ON-ORBIT IMAGES AND DISCUSSION

The panoramic camera was booted at 12:42 UTC on 2013 December 15. It successfully acquired the first color photo of the lander at 12:44:50 UTC.

Figure 18 is a photo of the upper part of the lander taken by the panoramic camera at working point D (8 m away from lunar rover). Figure 19 is a panoramic image of the lander, which is stitched from six images that show different parts of the lander image. Both of the images are clear, colorful, bright enough and have a large depth of field. The panoramic images show the lander's position and status very well.

Figure 20 is the panoramic images of the patrol area. As we can see, both near and far objects are clearly imaged. Through adjusting the exposure time automatically, the best contrast of images is obtained. During patrolling, the panoramic camera acquired a large number of useful images for further scientific research on the Moon (Dai et al. 2014). From 2013 December 15 to 2014 March 17, the panoramic camera successfully completed the expected scientific mission. It operated for a total of about 579 minutes, and took more than 780 images that could later be stitched with the expected image quality. During the entire process of operation, the temperature of the panoramic camera was between $-5°\mathrm{C}$ and $+40°\mathrm{C}$. That was within the designed working temperature range ($-20°\mathrm{C}\sim+45°\mathrm{C}$). This indicates that thermal control measures are rational and reliable. After going through three lunar nights with a low temperature of $-100°\mathrm{C}$, the image quality of the panoramic camera is still consistent with the requirements. This also demonstrates that the optical and structural system design is reasonable and reliable. In addition, the current in the electric cabinet varied within the normal range, which indicates that the electronic design is reasonable and reliable. A panoramic image of the lander after stitching had no flaw, which indicates the result of flat field correction is good. The color of the picture is normal and real, which indicates the matrix of color correction is correct. The on-orbit working status shows that all the engineering parameters associated with the panoramic camera are normal. Its image quality is satisfactory. All the performances satisfy the application requirements.

7 CONCLUSIONS

By choosing a simplified four piece optical lens system and highly integrated components, the CE-3 panoramic cameras demonstrate the advantages of the lightweight and miniaturized design of this instrument. Two kinds of thermal control measures are taken to allow the cameras to adapt to the wide range of environmental temperature on the Moon. Detailed ground testing experiments have been performed which verify that the cameras can operate normally and continuously in the harsh environment on the Moon for a long time. The good images taken on-orbit verify that the function, interface and performance of panoramic camera meet the user requirements very well. The panoramic images of the lander and patrol area provide a great amount of scientific data for lunar exploration.

Acknowledgements We wish to thank the referees for their constructive reports and all the participants for their great work in the CE-3 mission.

References

Dai, S.-W., Jia, Y.-Z., Zhang, B.-M., et al. 2014, Science China (Technological Sciences), 44, 361
Gao, Z.-Q., Yang, Z.-G., & Wang, X.-F. 2009, Remote Sensing and Aerial Photography, 4, 48
Hu, Y., & Zhang, Y. 2007, Spacecraft Recovery & Remote Sensing, 28, 54
Ip, Wing-Huen, Yan, J., Li, C.-L., et al. 2014, RAA (Research in Astronomy and Astrophysics), 14, 1511
Li, C.-L., Mu, L.-L., Zou, X.-D., et al. 2014, RAA (Research in Astronomy and Astrophysics), 14, 1514
Ouyang, Z.-Y. 2005, Intoduction to Lunar Science (Beijing: China Astronautic Publishing House)
Ouyang, Z.-Y. 2006, Bulletin of Chinese Academy of Sciences, 21, 370
Ren, X., Li, C.-L., Liu, J.-J., et al. 2014, RAA (Research in Astronomy and Astrophysics), 14, 1557
Sun, Z.-Z., Jia, Y., & Zhang, H. 2013, Science China (Technological Sciences), 56, 2702
Valous, N. A., Mendoza, F., Sun, D.-W., & Allen, P. 2009, Meat Science, 81, 132
Wang, X.-C., Pan, C., & Wu, X. 2014, Aerospace China, 1, 361